An homeotic post-transcriptional network controlled by the RNA-binding protein RBMX

Paola Zuccotti, Daniele Peroni, Valentina Potrich, Alessandro Quattrone, and Erik Dassi*

Centre for Integrative Biology (CIBIO), University of Trento, via Sommarive 9, 38123 Trento, TN, Italy.

*Correspondence to Erik Dassi: erik.dassi@unitn.it

Running head: RBMX controls homeotic genes expression

Keywords: *post-transcriptional regulation, 5'UTR, phylogenetic conservation, RNA-binding proteins, homeobox, RBMX*

Abstract

Post-transcriptional regulation (PTR) of gene expression is a powerful determinant of protein levels and cellular phenotypes. The 5' and 3' untranslated regions of the mRNA (UTRs) mediate this role through sequence and secondary structure elements bound by RNA-binding proteins (RBPs) and noncoding RNAs. While functional regions in the 3'UTRs have been extensively studied, the 5'UTRs are still relatively uncharacterized. To fill this gap, here we used a computational approach based on phylogenetic conservation to identify hyper-conserved elements in human 5'UTRs (5'HCEs). Our assumption, supported by the recovery of functionally characterized elements, was that 5'HCEs would represent evolutionarily stable and hence important PTR sites.

We identified over 5000 short, clustered 5'HCEs occurring in approximately 10% of human protein-coding genes. Among these, homeotic genes were highly enriched. Indeed, 52 of the 258 characterized homeotic genes contained at least one 5'HCE, including members of all four Hox clusters and several other families. Homeotic genes are essential transcriptional regulators. They drive body plan and neuromuscular development, and the role of PTR in their expression is mostly unknown. By integrating computational and experimental approaches we then identified the RBMX RNA-binding protein as the initiator of a post-transcriptional cascade regulating many such homeotic genes. RBMX is known to control its targets by modulating transcript abundance and alternative splicing. Adding to that, we observed translational control as a novel mode of regulation by this RBP.

This work thus establishes RBMX as a versatile master controller of homeotic genes and of the developmental processes they drive.

Introduction

Post-transcriptional control of gene expression (PTR) has recently emerged as a key determinant of protein levels and the consequent cell phenotypes (Schwanhäusser et al. 2011; Vogel et al. 2010). The two untranslated regions of the mRNA, the 5' and 3'UTR, mediate this role through sequence and secondary structure elements. These are bound by trans-factors such as RNA-binding proteins (RBPs) and noncoding RNAs (ncRNAs). These factors ultimately control the fate of a transcript by regulating its stability, localization, translation and influencing several other aspects of PTR (Glisovic et al. 2008; Noh et al. 2018; Bartel 2018). RBPs, in particular, are a major player in PTR, counting over 1500 human genes (Gerstberger et al. 2014). Their combined action forms a complex regulatory network of cooperative and competitive interactions (Dassi 2017).

Many works have focused on characterizing regulatory elements in 3'UTRs, mainly concerning mRNA stability and localization. However, less is known about functional regions in 5'UTRs. Which are the factors binding them, and which is their impact on the fate of the transcripts bearing them? A comprehensive catalog of functional regions in the 5'UTRs is still missing, thus hampering our ability to understand the mechanisms exploiting this regulatory hotspot. We and others have successfully compiled such a catalog in 3'UTRs, by exploiting the intuitive concept that evolutionarily conserved regions in mRNAs may be functional (Dassi et al. 2013; Bejerano 2004; McCormack et al. 2012; Reneker et al. 2012; Sathirapongsasuti et al. 2011). The 5' and 3'UTRs appear to have different functions (Mayr 2017; Hinnebusch et al. 2016), and are thus likely endowed with distinct profiles of cis-elements and targeting trans-factors. However, this phylogenetic approach is general.

Homeotic genes are a key class of developmental regulators (Philippidou and Dasen 2013; McGinnis and Krumlauf 1992; Olson and Rosenthal 1994). They are extremely conserved

73 throughout evolution and found in a range of species going from fungi to mammals (Holland
74 2013). These proteins, acting as transcription factors, are responsible for defining embryonic
75 regions identity along the anteroposterior and limb axes of vertebrates (Mallo et al. 2010;
76 Gehring 2012). Furthermore, homeotic genes have also been implicated in organ, neural and
77 muscular development (Philippidou and Dasen 2013; Zagozewski et al. 2014; Cambier et al.
78 2014). Much is known about how their expression is regulated at the transcriptional level (Mallo
79 and Alonso 2013). A few works have also focused on finding regulatory elements in homeotic
80 3'UTRs, uncovering several mechanisms mediated by RBPs (Nie et al. 2015; Fritz and
81 Stefanovic 2007; Pereira et al. 2013; Rogulja-Ortmann et al. 2014) and miRNAs (Yekta et al.
82 2004; Li et al. 2014; Wang et al. 2014). Concerning their 5'UTR, however, there is limited
83 evidence about the use of alternative transcription initiation sites (Regadas et al. 2013) and
84 regulation by RNA-binding proteins (Nie et al. 2015). Additionally, IRES-like elements found in
85 the 5'UTR of some Hox genes were observed to control ribosome specificity by recruiting
86 *RPL38 (Xue et al. 2015)*. Globally, we still know little about the homeotic genes 5'UTRs and the
87 post-transcriptional mechanisms acting on them.
88 Among the potential post-transcriptional regulators of these genes, *RBMX* is a scarcely studied
89 RBP whose inactivation has been previously associated with neuromuscular developmental
90 defects in *X. laevis* (Dichmann et al. 2008) and *D.rerio* (Tsend-Ayush et al. 2005). This suggests
91 it as a promising candidate regulator of homeotic genes. *RBMX,* also known as *hnRNP G*,
92 belongs to the *RBMY* gene family, of which it is an X-chromosome homolog. It contains a single
93 RRM domain and a C-terminal low-complexity region, by which it binds RNA. It was observed to
94 regulate splice site selection (Heinrich et al. 2009; Wang et al. 2011) and upregulate the
95 expression of the tumor suppressor *TXNIP* by an unspecified mechanism (Shin et al. 2008).
96 Further work found *RBMX* to be involved with the DNA-damage response (Adamson et al.
97 2012) and regulate centromere biogenesis (Cho et al. 2018; Matsunaga et al. 2012). Recently,
98 N6-methyladenosine marks were found to increase the accessibility of *RBMX* binding sites, thus

mediating its effect on its targets expression and splicing (Liu et al. 2017). Eventually, RBMX mutations were associated with the insurgence of an X-linked intellectual disability (XLID) syndrome associated with craniofacial dysmorphisms (Shashi et al. 2015).

We present here the analysis of hyper-conserved regions (HCEs) in 5'UTRs, based on a broad set of 44 vertebrates. Among the 5248 identified HCEs are several known and highly conserved regulatory sites, such as the iron response element (IRE), thus confirming the reliability of our approach. Through this potentially functional catalog of 5'UTR regions, we identified a group of homeotic genes controlled by the *RBMX* RNA-binding protein. We thus describe a novel regulatory network controlling homeotic genes at the post-transcriptional level, and a novel role for *RBMX* as a master translational controller of development.

Results

5'UTR HCEs are short and clustered phylogenetic footprints

To extract phylogenetically conserved regions from the 5'UTR of human mRNAs, we applied to the 5'UTRs the pipeline we previously described for 3'UTRs (Dassi et al. 2013). Briefly, we computed a per-nucleotide hyper-conservation score (HCS), ranging from 0 to 1. The HCS is the average of sequence conservation and the fraction of the phylogenetic tree covered by that UTR alignment (branch length score). A sliding-window approach was then used to find 5-nucleotides seeds with maximum conservation. Seeds were eventually extended upstream and downstream along the UTR while HCS held above a threshold of 0.85, thus extracting only highly conserved regions (see Methods). We term these regions 5' hyper-conserved elements (5'HCEs).

This approach led to the identification of 5248 HCEs (**Supplementary Table 1**), contained in

the 5'UTRs of 2737 transcripts coding for 2228 distinct genes. As shown in **Figure 1A**, these HCEs are mostly short, with an average length of 72 nucleotides and a median of 24 (minimum length 5 nucleotides, maximum 1542). 5'HCEs are thus 28% shorter on average than 3'UTR HCEs (Dassi et al. 2013). However, one should consider that 5'UTRs are also on average almost three times shorter than 3'UTRs (mean length of 455 nts for 5'UTR and 1282 nts for 3'UTRs). We then analyzed the nucleotide composition of 5'HCEs. **Figure 1B** shows the absence of imbalance in the frequencies of AU (typically enriched in 3'UTRs) and GC nucleotides. To further characterize the properties of 5'HCEs, we also observed their relative positional distribution. As can be seen in **Figure 1C**, almost a third of all 5'HCEs (1463/5248) are within 10 bases of another 5'HCE. This figure increases to almost 50% if we exclude 2028 isolated 5'HCEs (i.e., only 5'HCE found on that given 5'UTR), and only a few (155) are at least 50 nucleotides away from another 5'HCE. Globally, if considering a maximum distance of 20 nucleotides between 5'HCEs, 2672 out of 3220 non-isolated 5'HCEs (82%) are found in clusters. This suggests the prevalence of a clustered 5'HCE organization, a pattern also observed for 3'UTR HCEs (Dassi et al. 2013). Eventually, we analyzed the position of 5'HCEs in the containing UTRs. We observed them to be spread along the 5'UTR with a preference for its initial 10% (**Figure 1D**, 48% of HCEs). However, 27% of the 5'HCEs cover 95% or more of their 5'UTR, and thus start around its first bases. When excluding these, this positional preference decreases to 18% of the 5'HCEs only.

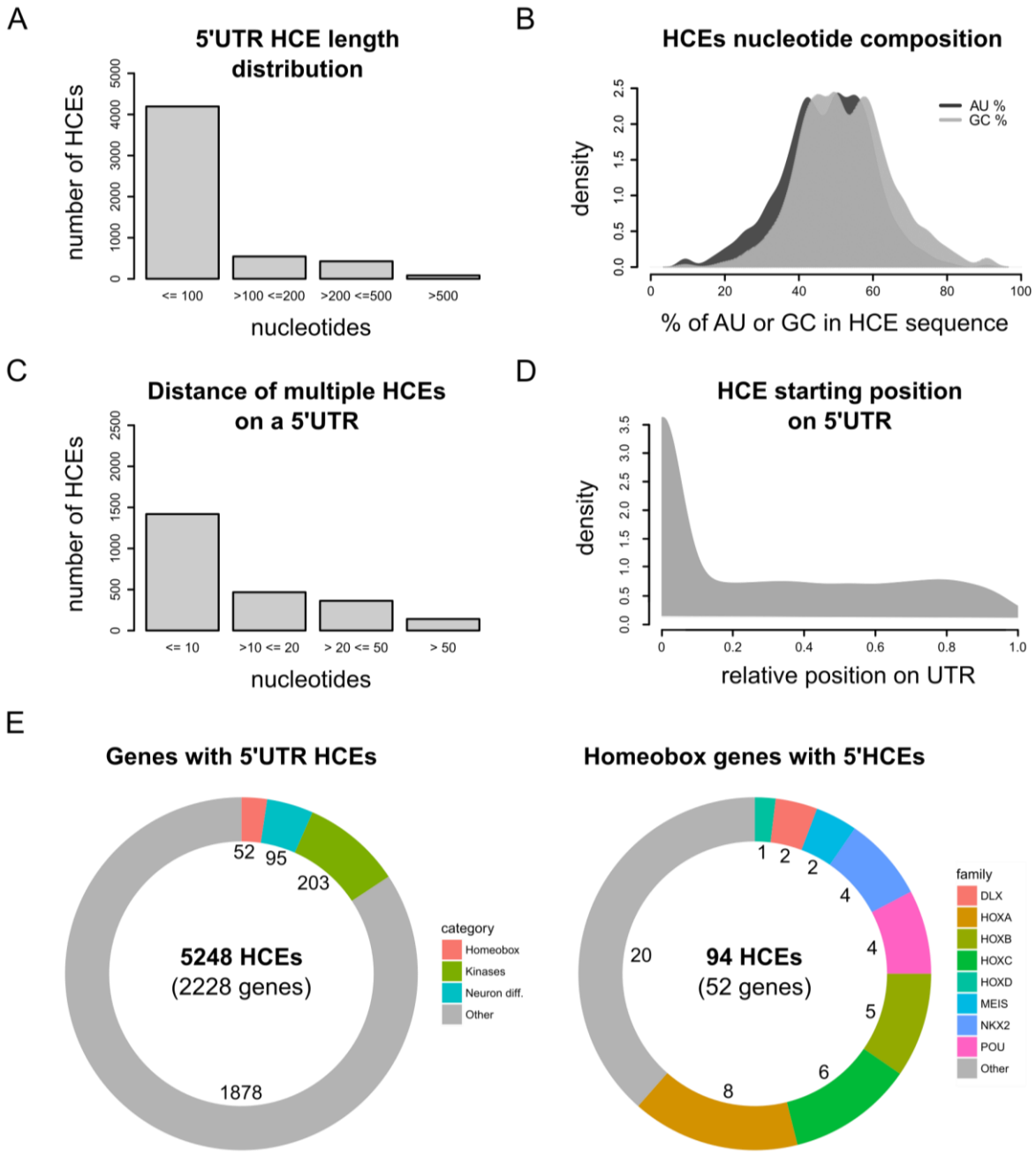

Figure 1: Homeotic genes are enriched in 5'UTR HCEs. A) shows the distribution of 5' hyper-conserved elements (5'HCEs) lengths, highlighting a striking majority of these to be shorter than 100 nucleotides. **B)** displays the density of AU and GC nucleotides frequencies in 5'HCEs, indicating that no significant bias in the composition can be observed. **C)** shows the distance between HCEs on 5'UTRs carrying more than one of these elements. There is a tendency for HCEs to be "clustered", i.e. in proximity to one another. **D)** displays the density of relative HCE

start positions on 5'UTRs (0 = UTR start, 1 = UTR end). HCEs are evenly distributed with the exception of an increased density in the first 10% of the UTR (representing less than 25% of all HCEs). **E)** shows the distribution of 5'HCEs by functional gene categories (left) and the abundance of homeotic families in HCE-containing homeobox genes (right). Numbers next to each category/family show the related number of genes.

We then sought to understand whether the identified 5'HCEs are representative of functional regions in the 5'UTRs. We thus searched in the AURA2 database (Dassi et al. 2014) for several 5'UTR cis-elements and RBP binding sites that were previously characterized and are known to be highly conserved. In particular, as shown in **Supplementary Figure 1**, we first considered two conserved iron response elements (IREs) (Gray et al. 1996; Hentze et al. 1987) in *ferritin* (*FTL*, **S1A**) and *aconitase 2* (*ACO2*, **S1B**) mRNAs. In both cases, an HCE is identified in that 5'UTR and contains the IRE. We then considered two conserved binding sites for the *LARP6* RBP, on *collagen alpha type 1* (*COL1A1*, **S1C**) (Cai et al. 2010) and *ornithine decarboxylase 1* (*ODC1*, **S1D**) (Manzella and Blackshear 1992) mRNA. While for *COL1A1* the identified HCE completely contains the *LARP6* binding site, in the case of *ODC1* the overlap is only partial but still present. Furthermore, 5'HCEs do not overlap with uORFs (Wethmar 2014) or IRESs (Yamamoto et al. 2017). Globally, these observations show that our HCE detection algorithm can identify functionally relevant phylogenetic footprints in 5'UTRs. Furthermore, it suggests 5'HCEs to be potential binding sites for RBPs.

Homeotic genes are enriched in 5'HCEs

We then annotated groups of functionally related genes among the 2228 containing one or more 5'HCEs. To do so, we performed a functional enrichment of genes, pathways and protein domain ontologies using DAVID (Huang et al. 2007). The results we obtained, as shown in **Figure 1E** and **Supplementary Table 2**, revealed the presence of three functional themes

178 endowed with high significance. The first theme, the homeobox, involves 52 genes representing
179 several families of these essential transcription factors (Ladam and Sagerström 2014).
180 Homeobox genes are responsible for developmental patterns (Gehring 2012; Philippidou and
181 Dasen 2013; Zagozewski et al. 2014) and are highly conserved throughout vertebrates, from the
182 fruit fly to human (Holland 2013). A second, functionally broader theme, regroups 95 genes
183 implicated in neuronal differentiation, some of which are also part of the previous theme. The
184 last theme is made up of 203 protein kinases. These include various kinase types (Ser/Thr, Tyr,
185 and others) affecting several signaling pathways (such as MAPK, NFKB, and others, as shown
186 in **Figure 1E**). Given the importance of homeotic genes in development and their high functional
187 coherence, we decided to focus our attention on this theme. We reasoned that these features
188 could allow us to trace a meaningful homeobox PTR network and investigate the related
189 regulatory mechanisms.
190 Among these 52 genes, whose 5'UTRs contain 94 HCEs, we can find members of all four Hox
191 clusters (eight *HOXA*, five *HOXB*, six *HOXC* and one *HOXD* genes). Other families are also
192 included, such as *NKX* and *POU* (four genes each), *MEIS* and *DLX* (two genes each). All these
193 proteins contain a homeobox domain and control developmental processes. Nevertheless,
194 specific functions such as pattern specification (25 genes), cell motion (10 genes) and neuronal
195 differentiation (20 genes) involve only a subset of these 52 genes. Homeobox 5'HCEs have a
196 median length of 28 nucleotides (ranging from 5 to 423 nucleotides). They are often clustered,
197 as 48/63 non-isolated HCEs are within 20 nucleotides of one another. **Supplementary Table 3**
198 and **4** present the complete list of genes composing this theme and their functional annotation.
199
200 **Homeotic 5'HCEs contain an RBMX-binding signature**
201 We thus asked ourselves whether this set of homeotic genes could be controlled by a common
202 regulatory mechanism through binding sites within their 5'HCEs. To identify such mechanism
203 we first performed an integrative motif search with DynaMIT (Dassi and Quattrone 2016),

combining a sequence search (using Weeder (Pavesi et al. 2004)) with an RNA secondary structure search (using RNAforester (Höchsmann et al. 2003)). Integration of the motifs identified by the two tools was done by clustering motifs co-occurring on the same sequences. Among the results, the best cluster included both sequence and secondary structure motifs shared by most homeotic 5'HCEs. The resulting motif, as shown in **Figure 2A**, is short, unstructured, and C-rich. Breaking down the consensus by its composing motifs reveals CGAC as shared by sequence search motifs of all length and CCAG as secondary structure search consensus.

Given this motif indication, we then proceeded by trying to understand which trans-factor may be binding it in order to exert a regulatory function on these homeotic genes. To this goal, we performed a search on known RBP binding motifs using the CISBP-RNA database (Ray et al. 2013). The results highlighted a protein, RBMX, having a binding consensus strikingly similar to the motifs found in these 5'HCEs (similarity score 93.5% and Pearson correlation 0.73). Its known consensus, derived by a SELEX experiment (Heinrich et al. 2009) is shown as a weblogo in the inset of **Figure 2A**.

To systematically map potential RBMX binding sites on homeotic genes 5'HCEs, we thus performed a pattern match analysis with the RBMX binding motif. The results, displayed in **Figure 2B**, show potential RBMX binding sites distributed throughout the homeotic genes 5'UTRs. These sites appear to be preferentially located in the proximity of each other (median 17 nts, average 41). Such sites distribution hints to a potential for homomultimeric RNA binding as previously observed for RBMX (Heinrich et al. 2009).

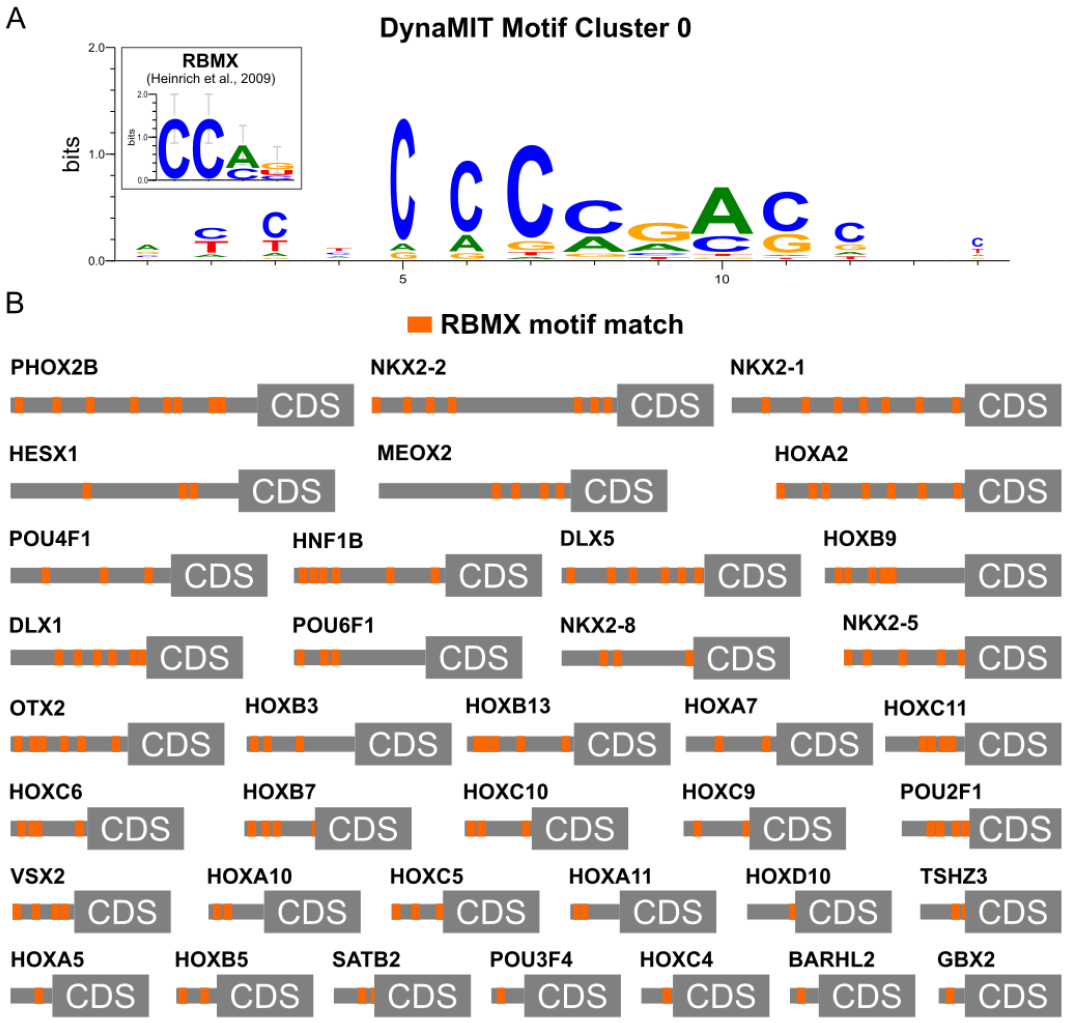

225

226 **Figure 2: Homeotic genes 5'HCEs contain an RBMX binding signature. A)** presents the
227 best motif cluster identified by DynaMIT in homeotic 5'HCEs by integrating sequence and
228 secondary structure motif searches. The leftmost inset displays the currently known binding
229 motif of RBMX as a WebLogo for comparison. **B)** displays matches for the RBMX binding motif
230 on the portion of homeotic genes 5'UTRs contained into an HCE. Matches, represented by
231 orange boxes, are clustered in 15 nucleotides windows (i.e. a single orange box may include
232 multiple matches within 15 nucleotides) for visualization purposes.

233

RBMX binds to homeotic genes mRNAs

The motif signature we detected in 5'HCEs of homeotic genes suggests that RBMX may contribute to the post-transcriptional regulation of their mRNAs. *RBMX* (also known as *HNRNPG*) is an RBP of the *RBMY* family, associated with neuromuscular developmental defects in *X. laevis* (Dichmann et al. 2008) and *D. rerio* (Tsend-Ayush et al. 2005), thus making it a promising candidate for post-transcriptional control of homeotic genes. To investigate this assumption, we first sought to confirm that RBMX is binding to homeotic mRNAs. We performed an RNA immunoprecipitation (RIP) assay followed by targeted RNA-sequencing in HEK293 cells, thus probing RBMX binding strength on the mRNAs of 50 genes. These included our 38 "core" homeotic genes, RBMX, two controls and additional members of families represented in the core genes. We computed the fold enrichment for each gene as the ratio between the normalized abundance in the RIP and the corresponding input samples. As shown in **Figure 3A,** we found 29/38 (76%) core homeotic genes to be enriched at least twofold in at least two of the three replicates (23/38 if using a fold enrichment threshold of four). Members of all four HOX clusters and other families such as *NKX* and *POU* were enriched. If considering all the 50 tested genes, 40 (80%) are enriched at least twofold in at least two replicates (32/50 if using a fold enrichment threshold of four). Among these, we find a known target of RBMX (Heinrich et al. 2009), FYN, which we used as positive control (2/3 replicates, average fold enrichment of 5.45). Our negative control, HNRNPM, is instead not enriched in any replicate (average fold enrichment of 1.43), as shown in **Figure 3B**. Remarkably, RBMX also binds to its cognate mRNA (all replicates, median fold enrichment 8.11), a frequent feature of RBPs (Dassi 2017). The list of bound genes can be found in **Supplementary Table 5**. Globally, this assay suggests that RBMX is indeed binding to a wide set of homeotic genes mRNAs. Thus, this RBP likely contributes to the post-transcriptional regulation of their expression.

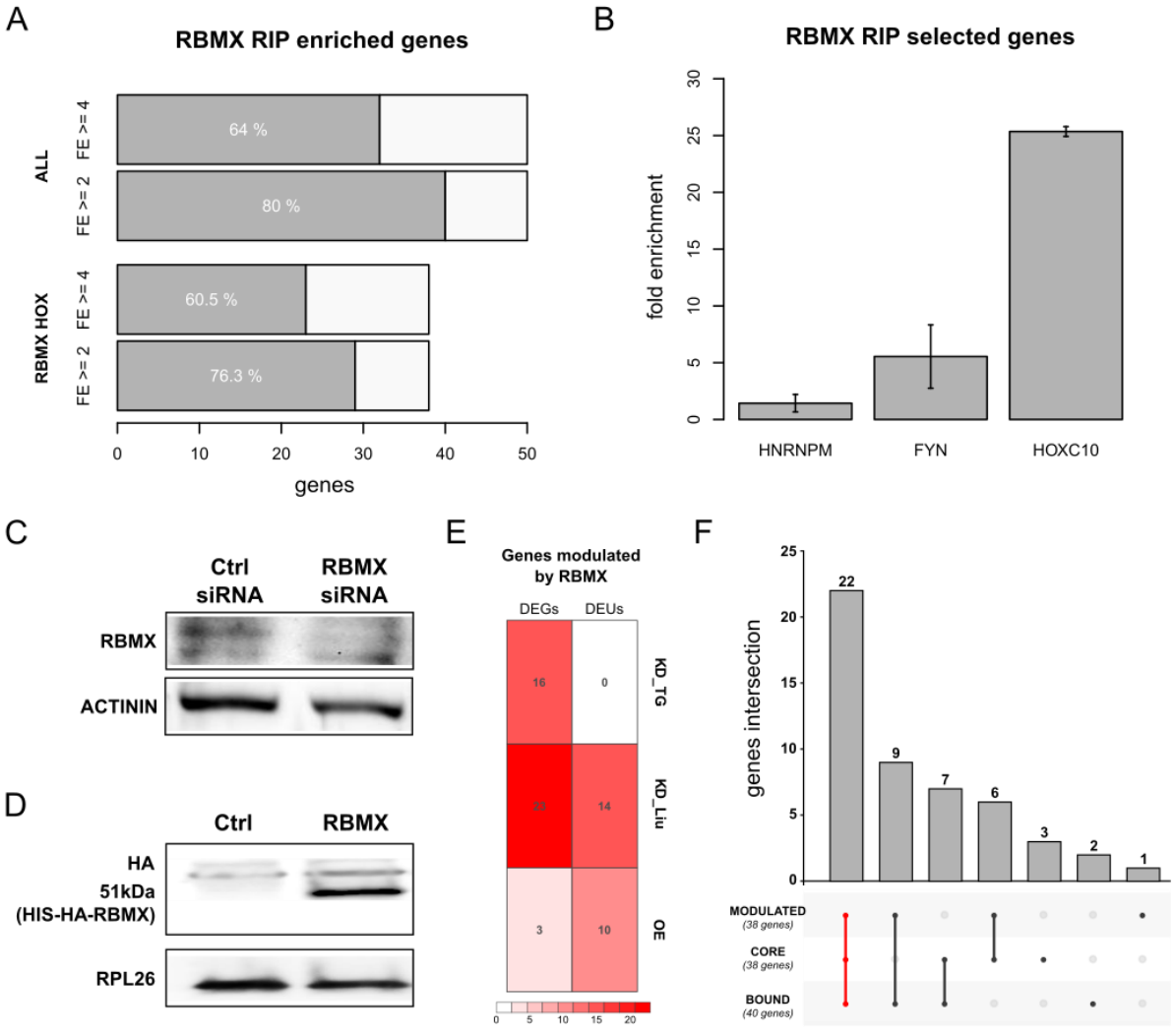

Figure 3. RBMX binds to homeotic genes mRNAs and controls their expression and splicing. A) shows the number of genes enriched in the RBMX RIP assay, at fold enrichment greater or equal than 2 (FE>=2) or 4 (FE>=4) in at least 2/3 replicates. Two sets of genes are considered, namely the core HOX genes set (RBMX HOX, 38 genes) and all tested genes (ALL, 50 genes). **B)** displays the fold enrichment in the RIP assay for the negative control (HNRNPM), the positive control (FYN), and one representative of the HOX core genes set (HOXC10). **C)**

RBMX western blot in HEK293 cells treated with control and RBMX siRNA, with Actinin used as reference protein. **D)** HA-tag western blot in control and RBMX-overexpressing HEK293 cells, with RPL26 used as reference protein. **E)** shows the number of differentially expressed (DEGs) and differential exon usage (DEUs) genes in our RBMX knock-down targeted RNA-seq (KD_TG), the Liu RBMX knock-down dataset (KD_Liu, (Liu et al. 2017)) and our RBMX overexpression dataset (OE). **F)** displays all the intersections for the set of genes modulated by RBMX (MODULATED, defined as the union of DEGs and DEUs), the core set of homeotic genes (CORE), and genes bound by RBMX as per the RIP assay (BOUND). The intersection of all three is highlighted in red.

RBMX controls homeotic genes mRNAs by post-transcriptional mechanisms

Given that RBMX binds to the mRNA of most homeotic genes containing a 5'HCE, we eventually sought to understand the impact this RBP has on their expression. To do so, we first used siRNAs to knock-down RBMX in HEK293 cells, reducing its protein level by 78% (**Figure 3C**, t-test p-value=0.00214). We thus performed a translatome profiling followed by targeted RNA-sequencing of total and polysomal fractions for the 50 genes which we previously tested by RNA immunoprecipitation. By this preliminary analysis, we identified 16 genes which were significantly upregulated at the polysomal level when silencing RBMX (log2 fold change >=1 and adjusted p-value <=0.1). Of these, 12 were part of the core homeotic genes and included members of all four HOX clusters, the DLX and POU families. However, replicates of samples at the total level were quite variable (average Spearman correlation=0.83). Furthermore, this assay does not allow to detect alternative splicing events, which can also be modulated by RBMX (Heinrich et al. 2009; Wang et al. 2011). So, to expand this analysis, we reanalyzed a recently published whole-transcriptome RNA-sequencing of HEK293 cells at the total level after RBMX knock-down (Liu et al. 2017). Eventually, we completed this dataset by overexpressing RBMX via a HIS-HA-tagged construct (**Figure 3D**) in the same cell type. These cells were then

297 subjected to translatome profiling followed by whole-transcriptome RNA-sequencing of the total
298 and polysomal fractions. Both datasets were analyzed to find differentially expressed genes
299 (DEGs) and differential exon usage (DEU) events (**Figure 3E**). DEGs were mostly in the knock-
300 down (23/50 genes, 6 up- and 7 down-regulated), with only 3/50 genes in overexpressed
301 samples (two up- and one down-regulated, 2 DEGs at both the total and polysomal level,
302 adjusted p-value <= 0.05). DEU events were more evenly distributed, with 10/50 genes affected
303 in the overexpressed (all upregulated exons, 6 at both the total and polysomal level) and 14/50
304 in the knock-down (4 up-, 3 down-regulated and 7 with both up- and down-regulated exons,
305 adjusted p-value <= 0.05). Eventually, we intersected all the datasets, also including the RIP
306 data to identify a consistently controlled set of homeotic genes. As shown in **Figure 3F**, 38/50
307 genes (76%) are controlled by RBMX, via alternative splicing or differential expression at the
308 total and polysomal level. Of these, 31 (62%) were also identified as bound by RBMX in the RIP
309 assay. Of the 38 core homeotic genes, 28 are modulated (73%), 22 of which (58%) were also
310 identified as bound by RBMX. Modulated genes in the core set include genes from all four HOX
311 clusters, the DLX, NKX2 and POU family. Lists of modulated genes for each dataset can be
312 found in **Supplementary Table 6** and **7**. Globally, this data indicates that RBMX extensively
313 controls the fate of homeotic genes mRNAs through complementary regulatory mechanisms.
314
315 **RBMX is a translational regulator**
316 RBMX controls its targets both by modulating their alternative splicing (Heinrich et al. 2009;
317 Wang et al. 2011; Liu et al. 2017) and transcript abundance (Liu et al. 2017; Shin et al. 2008).
318 The data we presented further confirm these findings. Furthermore, a few events (1 DEG and 4
319 DEUs) were observed at the polysomal level only, suggesting the possibility that RBMX may
320 also act as a translational regulator. To verify this possibility, we thus checked whether RBMX is
321 located in polysomes. We performed a polysomal profiling assay, followed by a fraction-by-
322 fraction western blot against RBMX and RPL26, a component of the ribosome. As shown in

323 **Figure 4A**, cytoplasmic RBMX is predominantly found in the polysomal fractions, with no
324 apparent increase in abundance in heavy polysomes with respect to lighter ones.
325 Eventually, we reasoned that observing RBMX associated with translation factors and ribosomal
326 proteins would further suggest it to be a translational regulator. To verify this possibility, we thus
327 analyzed known protein-protein interactions (PPIs) of RBMX. We collected experimentally
328 determined PPIs from the STRING (Szklarczyk et al. 2017) and IntAct (Orchard et al. 2014)
329 databases and performed a functional enrichment analysis of the resulting 83 RBMX interactors
330 (full list of genes and enriched terms in **Supplementary Table 8** and **9**). As shown in **Figure**
331 **4B**, mRNA splicing and processing are enriched (23 genes, adjusted Fisher test p=1.21E-21
332 and 2.6E-21), along with mRNA stabilization (4 genes, adjusted Fisher test p=6.3E-04). RBMX
333 interactors also include several translational regulators, represented by the “positive regulation
334 of translation” process (5 genes, adjusted Fisher test p=9.7E-04). In particular, RBM3 interacts
335 with RPL4 and is associated with polysomes through the 60S ribosomal subunit (Dresios et al.
336 2005), as is FXR2 (Siomi et al. 1996; Corbin et al. 1997). Eventually, CIRBP interacts with the
337 EIF4G1 translation initiation factor (Yang et al. 2006), and KHDRBS1 associates with
338 polysomes (Paronetto et al. 2006). Globally, these results show that RBMX can also act as a
339 translational regulator.
340

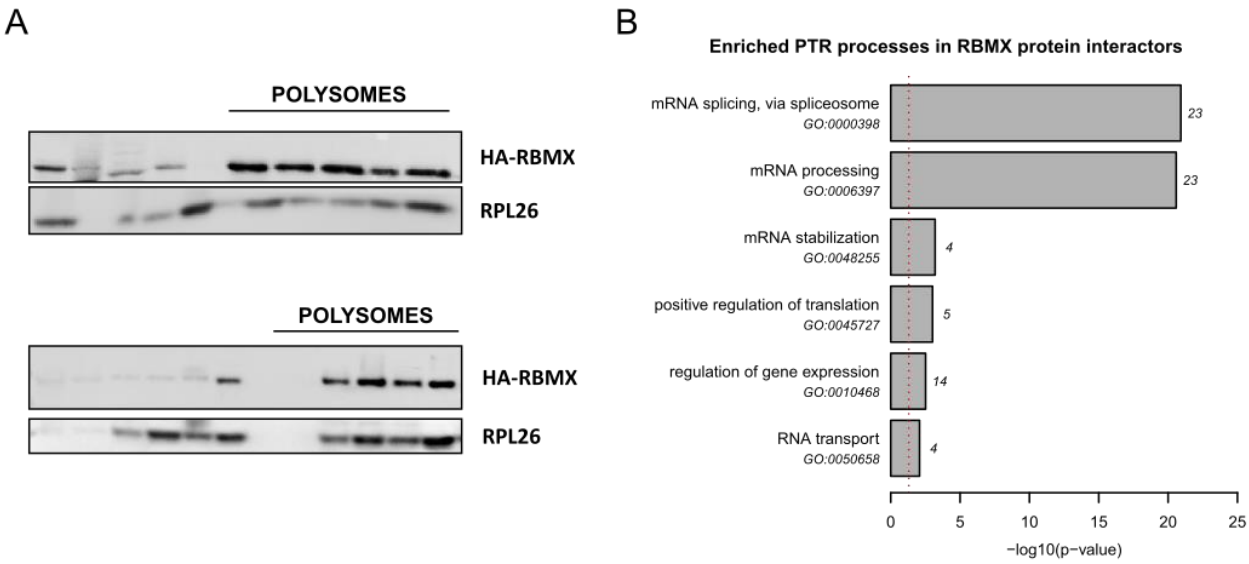

Figure 4. RBMX is a translational regulator. A) shows the distribution of RBMX on polysomes through a western blot of the fractions derived by polysomal profiling. The RPL26 ribosomal protein is used as positive control. **B)** displays post-transcriptional regulatory processes enriched in the set of RBMX protein-protein interactors. The enrichment p-value is shown on the x-axis as -log10(p-value). The number of RBMX interactors annotated to each process is instead shown next to the corresponding bar.

RBMX controls genes associated with XLID phenotypes

A frameshift deletion in the RBMX gene has been previously connected to the insurgence of an XLID syndrome associated with craniofacial dysmorphisms and intellectual disability, the Shashi syndrome (Shashi et al. 2015). We thus sought to check whether the homeotic genes we identified as modulated by RBMX could be involved with such phenotypes. To this end, we annotated the 22 homeotic genes in the core set which are bound and regulated by RBMX with three disease ontologies (see Methods). The results highlight several genes (HOXA2, NKX2-1, NKX2-5, POU2F1, and SATB2) associated with phenotypes compatible with this syndrome. These include mental retardation (SATB2), intellectual disability (NKX2-5), coarse facial

features (NKX2-1 and NKX2-5), bulbous nose (SATB2), underdeveloped supraorbital ridges (NKX2-5), orofacial cleft (POU2F1, SATB2, HOXA2) and mixed hearing impairment (HOXA2). If considering all 31 modulated and bound genes, HOXB3, HOXB5, and SIX6, associated with obesity and microphthalmia, are also included. Eventually, we expanded this analysis to phenotypes commonly associated with XLID syndromes in general (Stevenson et al. 2013). Further genes (DLX5, HOXC4, HOXC5) are associated with compatible phenotypes such as cardiac malformations, synostosis, hypospadias, and renal anomalies. The list of all annotations can be found in **Supplementary Table 10**. Globally, the regulatory activity of RBMX could thus be strongly associated with this group of diseases.

Discussion

In this work, we used a computational approach to extract phylogenetically hyper-conserved elements from the 5'UTR of human messenger RNAs (5'HCEs). We thus expanded the known catalog of regulatory mechanisms mediating the role of these regions in determining cell phenotypes. While much attention has been devoted to mapping functional elements in the 3'UTR, its 5' counterpart is still relatively uncharacterized. Our approach focused on extracting the most highly conserved regions, under the assumption that these would be evolutionary stable PTR sites of utmost importance.

The 5248 5'HCEs we identified are short regions occurring in around 10% of protein-coding genes, most often localized in proximity to one another. Given their prevalently clustered nature, 5'HCEs could represent loci of cooperation and competition between post-transcriptional regulatory factors. Through their interplay, these factors would ultimately determine the translation of the containing mRNAs. As 5'HCEs do not systematically overlap with uORFs or

IRESes, binding sites for the about 1500 human RNA-binding protein (RBP) genes are the likely orchestrators of such behaviors. Understanding how these mechanisms work and impact cell physiology and pathology will thus require further efforts towards the systematic mapping of RBP binding sites.

Among genes whose mRNA contain a 5'HCE, we identified a broad set of homeotic genes including members of all HOX clusters and several other related families. Homeotic genes are the prototypical class of conserved genes in metazoa, responsible for the development of the body plan, organs, and the nervous system (Holland 2013; Philippidou and Dasen 2013; Mallo et al. 2010). In that respect, they represent the ideal result of our algorithm, benchmarking its ability to identify truly conserved regions. While their transcriptional regulation is well characterized, we still lack a clear picture of how homeotic genes are controlled at the post-transcriptional level. In particular, only a few studies have explored the role of 5'UTRs in their regulation (Regadas et al. 2013; Nie et al. 2015; Xue et al. 2015). Identifying this set of 5'HCEs thus allowed us to improve our understanding of how PTR controls development through the 5'UTRs.

By applying de novo motif search combined with known RBP motifs matching we identified RBMX as a candidate post-transcriptional regulator of homeotic genes. Phenotypic studies have shown this protein, which is itself highly conserved, to affect neuromuscular development in *X. laevis* (Dichmann et al. 2008) and *D. rerio* (Tsend-Ayush et al. 2005). This evidence pointed to a possible role for RBMX as a controller of mRNAs of homeotic genes. We confirmed this hypothesis by a combination of RNA immunoprecipitation, knock-down, overexpression experiments, and sucrose-based cytoplasmic fractionation. This assays allowed us to probe multiple aspects of post-transcriptional regulation, including alternative splicing, mRNA stabilization, and translation. From this data, we found a possible new role for RBMX as a translational regulator. This finding establishes RBMX as a versatile controller of the mRNA, able to impact its lifecycle from alternative splicing to protein production. This flexibility may

have evolved to allow better control of processes requiring particularly fine tuning such as body plan establishment and neural development.

We have shown that RBMX regulates the mRNAs of many homeotic genes. However, other RBPs may also contribute to the post-transcriptional regulation of homeotic genes, possibly by cooperating or competing with RBMX. Further studies will thus be needed to complete this regulatory network.

Eventually, we explored the functional implications stemming from the role of RBMX. Which phenotypes does it drive? How would these be affected if its action was perturbed by genetic alterations typical of many diseases? An example is the Shashi syndrome (Shashi et al. 2015): a frameshift deletion in RBMX is associated with the onset of this XLID disease. Indeed, several of the homeotic targets of RBMX we identified are responsible for compatible phenotypes, such as mental retardation and cardiac malformations. Abnormal RBMX expression and function could thus lead to the insurgence of such syndromes through downstream altered expression of homeotic genes. Tuning the post-transcriptional networks RBMX controls could offer an important therapeutic opportunity for this class of diseases and, possibly, other developmental pathologies. Further studies are thus warranted to complete the characterization of this RBP as a master regulator of development.

Materials and Methods

5'HCE identification and characterization

Human 5'UTRs, the related 44-vertebrates alignment and sequence conservation scores (SCS) were downloaded from UCSC for the hg18 genome assembly (Tyner et al. 2017). Branch length score (BLS) was computed for each UTR as described in (Dassi et al. 2013), and composed at

435 equal weight with SCS to derive the hyper-conservation score (HCS). Then, a sliding-window
436 algorithm, starting with fully conserved 5-nucleotides seeds (HCS = 1.0) and expanding them
437 upstream and downstream until a minimum score threshold of 0.85 is reached, was applied to
438 the 5'UTRs, as described in (Dassi et al. 2013), to derive hyper-conserved elements (HCE).
439 HCE properties were then computed by custom Python scripts and plotted with R. Functional
440 enrichment in the set of genes containing HCEs in their 5'UTR was computed by DAVID (Huang
441 et al. 2007) using Gene Ontology (BP, MF, and CC parts) and protein domain ontologies
442 (INTERPRO, PFAM, and SMART).
443
444 **Motif analysis**
445 De novo motif search was performed on the sequences of 5'HCEs from homeotic genes using
446 DynaMIT (Dassi and Quattrone 2016), configured to use two search tools: Weeder (Pavesi et al.
447 2004) for sequence motifs (lengths 6, 8, 10 and 12 nts with 1, 2, 3 and 4 mismatches allowed
448 resp.; at least 25% of the sequences containing the motif) and RNAforester (Höchsmann et al.
449 2003) for secondary structure motifs (multiple alignment and local search modes). The selected
450 motif integration strategy was "co-occurrence", which computes the co-occurrence score
451 between motifs pairs as the Jaccard similarity of the mutual presence of both motifs on each
452 sequence. This measure thus allows finding motifs which co-regulate the same sequences set.
453 The best motif from DynaMIT result was selected, and only positions with at least ten supporting
454 sequences were kept. This resulted in trimming the 5' and 3' ends of the integrated motif. These
455 trimmed ends represented lowly-supported, more "peripheral" individual motifs with respect to
456 the core part consistently shared by multiple motifs.
457 The PWMs for a set of 193 RBPs were obtained from the CISBP-RNA database (Ray et al.
458 2013). Pearson correlation between the CISBP-RNA PWMs and the motif identified by DynaMIT
459 were computed by the TFBSTools R package (Tan and Lenhard 2016). The RBMX PWM
460 obtained from CISBP-RNA was matched against the sequences of 5'HCEs from homeotic

461 genes using a custom Python script and the Biopython library (Cock et al. 2009). Only PWMs at
462 least four nucleotides long were used, and only matches with a score greater than 70% were
463 considered.
464
465 **Cell culture and transfection**
466 HEK293 cells were cultured in DMEM with 10% FBS, 100 U/ml penicillin-streptomycin and 0.01
467 mM l-glutamine (Gibco, Waltham, MA). Cultures were maintained at 37°C in a 5% CO2
468 incubator.
469
470 **RBMX knock-down and overexpression**
471 We performed RBMX knock-down as described in (Matsunaga et al. 2012). Briefly, we used
472 RBMX siRNA-1 (5'-UCAAGAGGAUAUAGCGAUATT-3') and RBMX siRNA-2 (5'-
473 CGGAUAUGGUGGAAGUCGAUU-3') for RBMX knock-down, and negative control siRNA S5C-
474 060 (Cosmo Bio, Tokyo). 1.5×10^6 HEK293 cells were seeded into two 10-cm Petri dishes and
475 transfected with a mixture of both siRNA at 25nM using Lipofectamine 2000.
476 Full-length RBMX was amplified by PCR using HeLa cells cDNA and the following primers: Fw:
477 5' GAGGCGATCGCCGTTGAAGCAGATCGCCCAGGAA 3' and Rv: 5'
478 GCGACGCGTCTAGTATCTGCTTCTGCCTCCC 3'. The amplified fragment was digested with
479 the SgfI and MluI restriction enzymes and cloned into the pCMV6-AN-His-HA plasmid
480 (PS100017, OriGene, Rockville, MD) to obtain the pCMV6-HIS-HA-RBMX vector, expressing
481 the gene fused with an amino-terminal polyhistidine (His) tag and a hemagglutinin (HA) epitope.
482 The construct was confirmed by sequencing. 1.5×10^6 HEK293 cells were seeded into two 10-
483 cm Petri dishes and transiently transfected using Lipofectamine 2000 (Invitrogen, Waltham, MA)
484 with 2µg of pCMV6-HIS-HA-RBMX or the mock empty vector as control. Total and polysomal
485 RNA extractions were performed 48h post-transfection. All the experiments were run at least in
486 biological triplicate.

487

488 **RNA immunoprecipitation**

489 Ribonucleoprotein immunoprecipitation (RIP) was performed in three biological replicates using
490 lysates of human HEK293 cells transfected with pCMV6-HIS-HA-RBMX or with the mock empty
491 vector. Cell extracts were resuspended in NT2 buffer (50 mM Tris–HCl pH 7.4, 150 mM NaCl, 1
492 mM MgCl2, 0.05% NP-40 supplemented with fresh 200 U RNase Out, 20 mM EDTA and a
493 protease inhibitor cocktail), chilled at 4°C. Anti-HA magnetic beads (Pierce, Waltham, MA, USA)
494 were saturated in the NT2 buffer (adding 5% BSA for 1h at 4°C), then added to lysates. The
495 immunoprecipitation was performed overnight at 4°C in gentle rotation condition. Eventually, the
496 immunoprecipitate was washed four times with NT2 and resuspended in the same buffer. RNA
497 extraction was performed from 10% of the volume of both the input and the immunoprecipitate
498 samples, using TRIzol (Invitrogen, Carlsbad, CA, USA). Sequencing libraries were then
499 prepared following the manufacturer's instructions as described below. FYN mRNA was used as
500 the positive control and HNRNPM as the negative control (Heinrich et al. 2009).

501

502 **Polysomal fractionation and RNA extraction**

503 Cells were incubated for 4min with 10 µg/ml cycloheximide at 37°C to block translational
504 elongation. Cells were washed with PBS + 10 µg/ml cycloheximide, scraped on the plate with
505 300 µl lysis buffer (10 mM NaCl, 10 mM MgCl2, 10 mM Tris-HCl, pH 7.5, 1% Triton X-100, 1%
506 sodium deoxycholate, 0.2 U/µl RNase inhibitor [Fermentas Burlington, CA], 10 µg/ml
507 cycloheximide, 5 U/mL DNase I [New England Biolabs, Hitchin, UK] and 1 mM DTT) and
508 transferred to a tube. Nuclei and cellular debris were removed by centrifugation for 5min at
509 13,000g at 4°C. The lysate was layered on a linear sucrose gradient (15-50% sucrose (w/v), in
510 30 mM Tris–HCl at pH 7.5, 100 mM NaCl, 10 mM MgCl2) and centrifuged in an SW41Ti rotor
511 (Beckman Coulter, Indianapolis, IN) at 4°C for 100min at 180,000g. Ultracentrifugation
512 separates polysomes by the sedimentation coefficient of macromolecules: gradients are then

fractionated and mRNAs in active translation, corresponding to polysome-containing fractions, separated from untranslated mRNAs. Fractions of 1 mL volume were collected with continuous monitoring absorbance at 254 nm. Total RNA was obtained by pooling together 20% of each fraction. To extract RNA, polysomal and total fractions were treated with 0.1 mg/ml proteinase K (Euroclone, Italy) for 2h at 37°C. After phenol-chloroform extraction and isopropanol precipitation, RNA was resuspended in 30 µl of RNase-free water. RNA integrity was assessed by an Agilent Bioanalyzer and RNA quantified by a Qubit (Life Technologies, Waltham, MA).

Protein extraction and Western blots

10% of each fraction collected from sucrose gradient fractionation was pooled (for knock-down and overexpression validation) or processed separately (for the RBMX polysomes distribution assay) to extract proteins using TCA/acetone precipitation. Proteins were resolved on 15% SDS-PAGE, transferred to nitrocellulose membrane and immunoblotted with RBMX (Abcam, Cambridge, UK), HA (Bethyl Laboratories, Montgomery, TX) and RPL26 antibodies (Abcam, Cambridge, UK). Blots were processed by an ECL Prime detection kit (Amersham Biosciences).

RNA-seq

For the RNA immunoprecipitation and the RBMX knock-down samples, after total and polysomal RNA extraction, 500ng RNA of each sample were used to prepare libraries according to the manufacturer's protocol, using a TruSeq Targeted RNA Custom Panel Kit (Illumina, San Diego, CA). Sequencing was performed with a 50-cycle MiSeq Reagent Kit v2 (Illumina, San Diego, CA) on a MiSeq machine. For the overexpression samples, after total and polysomal RNA extraction, 500ng RNA of each sample were used to prepare libraries according to the manufacturer's protocol, using the TruSeq RNA Sample Prep Kit (Illumina, San Diego, CA). Sequencing was performed on six lanes at 2x100bp on a HiSeq 2500 machine. Sequencing was performed at least in triplicate for each sample.

539

540 **RNA-seq data analysis**

541 Reads were pre-processed with trimmomatic (Bolger et al.), trimming bases having quality lower
542 than Q30 and removing sequencing adapters. Remaining reads were aligned to the human
543 genome hg38 assembly with bowtie2 (Langmead and Salzberg 2012) for the targeted
544 sequencing, and with STAR for the other datasets (Dobin et al. 2013). Read counts for each
545 gene determined using the Gencode v27 annotation (Harrow et al. 2012), and normalized by the
546 sequencing depth of the libraries. Fold enrichment for RNA immunoprecipitation were computed
547 as the ratio of enrichment of (RIP vs. input samples for the RBMX IP) over (RIP vs. input
548 samples for the HA IP), for each replicate. For the targeted RNA-seq of RBMX knock-down
549 samples, samples with less than 500 mapped reads (less than 10 mapped reads per targeted
550 gene) were discarded, and differences in expression were computed by a Wilcoxon test, as this
551 type of library (probing only 50 genes) does not fit the assumptions of commonly used
552 differential expression determination methods. For overexpression and the published RBMX
553 knock-down we obtained from (Liu et al. 2017), differential expression was computed with
554 DESeq2 (Love et al. 2014), while differential exon usage was obtained by DEXseq (Anders et
555 al. 2012) (adjusted p-value <=0.05 for both analyses). Functional annotation was performed by
556 Enrichr (Chen et al.) on Gene Ontology or disease ontologies (OMIM disease, Jensen disease,
557 and Human Phenotype Ontology) annotations.

558

559 **Data availability**

560 Datasets can be found in GEO with ID GSE118383 (RBMX RIP targeted RNA-seq and RBMX
561 knock-down targeted RNA-seq) and GSE68990 (RBMX overexpression RNA-seq).

562

563

Supplemental figures

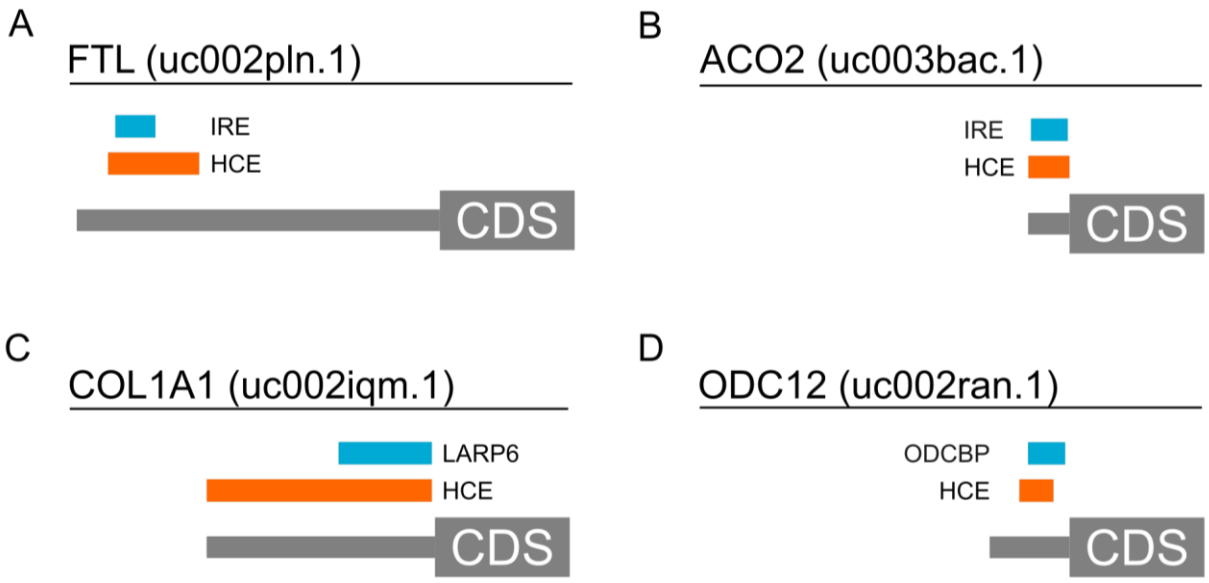

Supplementary Figure 1: 5'HCEs contain conserved binding sites and cis-elements. The figure displays four example of functional regions retrieved by the HCE identification algorithm in 5'UTRs. **A)** a known, conserved iron response element (IRE) in the 5'UTR of ferritin (FTL) is fully contained in an HCE. **B)** a known, conserved iron response element (IRE) in the 5'UTR of aconitase 2 (ACO2) is fully contained in an HCE. **C)** a conserved binding site for LARP6 in the 5'UTR of collagen alpha type 1 (COL1A1) is fully contained into an HCE. **D)** a conserved binding site for ODCBP in the 5'UTR of ornithine decarboxylase 1 (ODC1) is partially overlapping with an HCE.

Acknowledgments

We thank Veronica De Sanctis and Roberto Bertorelli (NGS Facility, Centre for Integrative Biology and LaBSSAH, University of Trento) for performing NGS sequencing.

References

Adamson B, Smogorzewska A, Sigoillot FD, King RW, Elledge SJ. 2012. A genome-wide homologous recombination screen identifies the RNA-binding protein RBMX as a component of the DNA-damage response. *Nat Cell Biol* **14**: 318–328.

Anders S, Reyes A, Huber W. 2012. Detecting differential usage of exons from RNA-seq data. *Genome Res* **22**: 2008–2017.

Bartel DP. 2018. Metazoan MicroRNAs. *Cell* **173**: 20–51.

Bejerano G. 2004. Ultraconserved Elements in the Human Genome. *Science* **304**: 1321–1325.

Cai L, Fritz D, Stefanovic L, Stefanovic B. 2010. Binding of LARP6 to the conserved 5' stem-loop regulates translation of mRNAs encoding type I collagen. *J Mol Biol* **395**: 309–326.

Cambier L, Plate M, Sucov HM, Pashmforoush M. 2014. Nkx2-5 regulates cardiac growth through modulation of Wnt signaling by R-spondin3. *Development* **141**: 2959–2971.

Cho Y, Ideue T, Nagayama M, Araki N, Tani T. 2018. RBMX is a component of the centromere noncoding RNP complex involved in cohesion regulation. *Genes Cells* **23**: 172–184.

Cock PJA, Antao T, Chang JT, Chapman BA, Cox CJ, Dalke A, Friedberg I, Hamelryck T, Kauff F, Wilczynski B, et al. 2009. Biopython: freely available Python tools for computational molecular biology and bioinformatics. *Bioinformatics* **25**: 1422–1423.

Corbin F, Bouillon M, Fortin A, Morin S, Rousseau F, Khandjian EW. 1997. The fragile X mental

603 retardation protein is associated with poly(A)+ mRNA in actively translating polyribosomes.
604 *Hum Mol Genet* **6**: 1465–1472.
605 Dassi E. 2017. Handshakes and Fights: The Regulatory Interplay of RNA-Binding Proteins.
606 *Front Mol Biosci* **4**: 67.
607 Dassi E, Quattrone A. 2016. DynaMIT: the dynamic motif integration toolkit. *Nucleic Acids Res*
608 **44**: e2.
609 Dassi E, Re A, Leo S, Tebaldi T, Pasini L, Peroni D, Quattrone A. 2014. AURA 2. *Translation* **2**:
610 e27738.
611 Dassi E, Zuccotti P, Leo S, Provenzani A, Assfalg M, D'Onofrio M, Riva P, Quattrone A. 2013.
612 Hyper conserved elements in vertebrate mRNA 3'-UTRs reveal a translational network of
613 RNA-binding proteins controlled by HuR. *Nucleic Acids Res* **41**: 3201–3216.
614 Dichmann DS, Fletcher RB, Harland RM. 2008. Expression cloning in Xenopus identifies RNA-
615 binding proteins as regulators of embryogenesis and Rbmx as necessary for neural and
616 muscle development. *Dev Dyn* **237**: 1755–1766.
617 Dobin A, Davis CA, Schlesinger F, Drenkow J, Zaleski C, Jha S, Batut P, Chaisson M, Gingeras
618 TR. 2013. STAR: ultrafast universal RNA-seq aligner. *Bioinformatics* **29**: 15–21.
619 Dresios J, Aschrafi A, Owens GC, Vanderklish PW, Edelman GM, Mauro VP. 2005. Cold stress-
620 induced protein Rbm3 binds 60S ribosomal subunits, alters microRNA levels, and
621 enhances global protein synthesis. *Proc Natl Acad Sci U S A* **102**: 1865–1870.
622 Fritz D, Stefanovic B. 2007. RNA-binding protein RBMS3 is expressed in activated hepatic
623 stellate cells and liver fibrosis and increases expression of transcription factor Prx1. *J Mol*
624 *Biol* **371**: 585–595.
625 Gehring WJ. 2012. The animal body plan, the prototypic body segment, and eye evolution. *Evol*
626 *Dev* **14**: 34–46.
627 Gerstberger S, Hafner M, Tuschl T. 2014. A census of human RNA-binding proteins. *Nat Rev*
628 *Genet* **15**: 829–845.

629 Glisovic T, Bachorik JL, Yong J, Dreyfuss G. 2008. RNA-binding proteins and post-
630 transcriptional gene regulation. *FEBS Lett* **582**: 1977–1986.
631 Gray NK, Pantopoulos K, Dandekar T, Ackrell BA, Hentze MW. 1996. Translational regulation of
632 mammalian and Drosophila citric acid cycle enzymes via iron-responsive elements. *Proc*
633 *Natl Acad Sci U S A* **93**: 4925–4930.
634 Harrow J, Frankish A, Gonzalez JM, Tapanari E, Diekhans M, Kokocinski F, Aken BL, Barrell D,
635 Zadissa A, Searle S, et al. 2012. GENCODE: the reference human genome annotation for
636 The ENCODE Project. *Genome Res* **22**: 1760–1774.
637 Heinrich B, Zhang Z, Raitskin O, Hiller M, Benderska N, Hartmann AM, Bracco L, Elliott D, Ben-
638 Ari S, Soreq H, et al. 2009. Heterogeneous nuclear ribonucleoprotein G regulates splice
639 site selection by binding to CC(A/C)-rich regions in pre-mRNA. *J Biol Chem* **284**: 14303–
640 14315.
641 Hentze MW, Rouault TA, Caughman SW, Dancis A, Harford JB, Klausner RD. 1987. A cis-
642 acting element is necessary and sufficient for translational regulation of human ferritin
643 expression in response to iron. *Proc Natl Acad Sci U S A* **84**: 6730–6734.
644 Hinnebusch AG, Ivanov IP, Sonenberg N. 2016. Translational control by 5'-untranslated regions
645 of eukaryotic mRNAs. *Science* **352**: 1413–1416.
646 Höchsmann M, Töller T, Giegerich R, Kurtz S. 2003. Local similarity in RNA secondary
647 structures. *Proc IEEE Comput Soc Bioinform Conf* **2**: 159–168.
648 Holland PWH. 2013. Evolution of homeobox genes. *Wiley Interdiscip Rev Dev Biol* **2**: 31–45.
649 Huang DW, Sherman BT, Tan Q, Collins JR, Alvord WG, Roayaei J, Stephens R, Baseler MW,
650 Lane HC, Lempicki RA. 2007. The DAVID Gene Functional Classification Tool: a novel
651 biological module-centric algorithm to functionally analyze large gene lists. *Genome Biol* **8**:
652 R183.
653 Ladam F, Sagerström CG. 2014. Hox regulation of transcription: more complex(es). *Dev Dyn*
654 **243**: 4–15.

655 Langmead B, Salzberg SL. 2012. Fast gapped-read alignment with Bowtie 2. *Nat Methods* **9**:
656 357–359.
657 Li T, Lu YY, Zhao XD, Guo HQ, Liu CH, Li H, Zhou L, Han YN, Wu KC, Nie YZ, et al. 2014.
658 MicroRNA-296-5p increases proliferation in gastric cancer through repression of Caudal-
659 related homeobox 1. *Oncogene* **33**: 783–793.
660 Liu N, Zhou KI, Parisien M, Dai Q, Diatchenko L, Pan T. 2017. N6-methyladenosine alters RNA
661 structure to regulate binding of a low-complexity protein. *Nucleic Acids Res* **45**: 6051–6063.
662 Love MI, Huber W, Anders S. 2014. Moderated estimation of fold change and dispersion for
663 RNA-seq data with DESeq2. *Genome Biol* **15**: 550.
664 Mallo M, Alonso CR. 2013. The regulation of Hox gene expression during animal development.
665 *Development* **140**: 3951–3963.
666 Mallo M, Wellik DM, Deschamps J. 2010. Hox genes and regional patterning of the vertebrate
667 body plan. *Dev Biol* **344**: 7–15.
668 Manzella JM, Blackshear PJ. 1992. Specific protein binding to a conserved region of the
669 ornithine decarboxylase mRNA 5'-untranslated region. *J Biol Chem* **267**: 7077–7082.
670 Matsunaga S, Takata H, Morimoto A, Hayashihara K, Higashi T, Akatsuchi K, Mizusawa E,
671 Yamakawa M, Ashida M, Matsunaga TM, et al. 2012. RBMX: a regulator for maintenance
672 and centromeric protection of sister chromatid cohesion. *Cell Rep* **1**: 299–308.
673 Mayr C. 2017. Regulation by 3′-Untranslated Regions. *Annu Rev Genet* **51**: 171–194.
674 McCormack JE, Faircloth BC, Crawford NG, Gowaty PA, Brumfield RT, Glenn TC. 2012.
675 Ultraconserved elements are novel phylogenomic markers that resolve placental mammal
676 phylogeny when combined with species-tree analysis. *Genome Res* **22**: 746–754.
677 McGinnis W, Krumlauf R. 1992. Homeobox genes and axial patterning. *Cell* **68**: 283–302.
678 Nie J, Jiang M, Zhang X, Tang H, Jin H, Huang X, Yuan B, Zhang C, Lai JC, Nagamine Y, et al.
679 2015. Post-transcriptional Regulation of Nkx2-5 by RHAU in Heart Development. *Cell Rep*
680 **13**: 723–732.

681 Noh JH, Kim KM, McClusky WG, Abdelmohsen K, Gorospe M. 2018. Cytoplasmic functions of
682 long noncoding RNAs. *Wiley Interdiscip Rev RNA*. http://dx.doi.org/10.1002/wrna.1471.
683 Olson EN, Rosenthal N. 1994. Homeobox genes and muscle patterning. *Cell* **79**: 9–12.
684 Orchard S, Ammari M, Aranda B, Breuza L, Briganti L, Broackes-Carter F, Campbell NH,
685 Chavali G, Chen C, del-Toro N, et al. 2014. The MIntAct project--IntAct as a common
686 curation platform for 11 molecular interaction databases. *Nucleic Acids Res* **42**: D358–63.
687 Paronetto MP, Zalfa F, Botti F, Geremia R, Bagni C, Sette C. 2006. The nuclear RNA-binding
688 protein Sam68 translocates to the cytoplasm and associates with the polysomes in mouse
689 spermatocytes. *Mol Biol Cell* **17**: 14–24.
690 Pavesi G, Mereghetti P, Mauri G, Pesole G. 2004. Weeder Web: discovery of transcription
691 factor binding sites in a set of sequences from co-regulated genes. *Nucleic Acids Res* **32**:
692 W199–203.
693 Pereira B, Sousa S, Barros R, Carreto L, Oliveira P, Oliveira C, Chartier NT, Plateroti M,
694 Rouault J-P, Freund J-N, et al. 2013. CDX2 regulation by the RNA-binding protein MEX3A:
695 impact on intestinal differentiation and stemness. *Nucleic Acids Res* **41**: 3986–3999.
696 Philippidou P, Dasen JS. 2013. Hox genes: choreographers in neural development, architects of
697 circuit organization. *Neuron* **80**: 12–34.
698 Ray D, Kazan H, Cook KB, Weirauch MT, Najafabadi HS, Li X, Gueroussov S, Albu M, Zheng
699 H, Yang A, et al. 2013. A compendium of RNA-binding motifs for decoding gene regulation.
700 *Nature* **499**: 172–177.
701 Regadas I, Matos MR, Monteiro FA, Gómez-Skarmeta JL, Lima D, Bessa J, Casares F,
702 Reguenga C. 2013. Several cis-regulatory elements control mRNA stability, translation
703 efficiency, and expression pattern of Prrxl1 (paired related homeobox protein-like 1). *J Biol*
704 *Chem* **288**: 36285–36301.
705 Reneker J, Lyons E, Conant GC, Pires JC, Freeling M, Shyu C-R, Korkin D. 2012. Long
706 identical multispecies elements in plant and animal genomes. *Proc Natl Acad Sci U S A*

109: E1183–91.

Rogulja-Ortmann A, Picao-Osorio J, Villava C, Patraquim P, Lafuente E, Aspden J, Thomsen S, Technau GM, Alonso CR. 2014. The RNA-binding protein ELAV regulates Hox RNA processing, expression and function within the Drosophila nervous system. *Development* **141**: 2046–2056.

Sathirapongsasuti JF, Sathira N, Suzuki Y, Huttenhower C, Sugano S. 2011. Ultraconserved cDNA segments in the human transcriptome exhibit resistance to folding and implicate function in translation and alternative splicing. *Nucleic Acids Res* **39**: 1967–1979.

Schwanhäusser B, Busse D, Li N, Dittmar G, Schuchhardt J, Wolf J, Chen W, Selbach M. 2011. Global quantification of mammalian gene expression control. *Nature* **473**: 337–342.

Shashi V, Xie P, Schoch K, Goldstein DB, Howard TD, Berry MN, Schwartz CE, Cronin K, Sliwa S, Allen A, et al. 2015. The RBMX gene as a candidate for the Shashi X-linked intellectual disability syndrome. *Clin Genet* **88**: 386–390.

Shin K-H, Kim RH, Kim RH, Kang MK, Park N-H. 2008. hnRNP G elicits tumor-suppressive activity in part by upregulating the expression of Txnip. *Biochem Biophys Res Commun* **372**: 880–885.

Siomi MC, Zhang Y, Siomi H, Dreyfuss G. 1996. Specific sequences in the fragile X syndrome protein FMR1 and the FXR proteins mediate their binding to 60S ribosomal subunits and the interactions among them. *Mol Cell Biol* **16**: 3825–3832.

Stevenson RE, Schwartz CE, Rogers RC. 2013. Malformations among the X-linked intellectual disability syndromes. *Am J Med Genet A* **161A**: 2741–2749.

Szklarczyk D, Morris JH, Cook H, Kuhn M, Wyder S, Simonovic M, Santos A, Doncheva NT, Roth A, Bork P, et al. 2017. The STRING database in 2017: quality-controlled protein-protein association networks, made broadly accessible. *Nucleic Acids Res* **45**: D362–D368.

Tan G, Lenhard B. 2016. TFBSTools: an R/bioconductor package for transcription factor binding site analysis. *Bioinformatics* **32**: 1555–1556.

733 Tsend-Ayush E, O'Sullivan LA, Grützner FS, Onnebo SMN, Lewis RS, Delbridge ML, Marshall
734 Graves JA, Ward AC. 2005. RBMX gene is essential for brain development in zebrafish.
735 *Dev Dyn* **234**: 682–688.
736 Tyner C, Barber GP, Casper J, Clawson H, Diekhans M, Eisenhart C, Fischer CM, Gibson D,
737 Gonzalez JN, Guruvadoo L, et al. 2017. The UCSC Genome Browser database: 2017
738 update. *Nucleic Acids Res* **45**: D626–D634.
739 Vogel C, Abreu R de S, Ko D, Le S-Y, Shapiro BA, Burns SC, Sandhu D, Boutz DR, Marcotte
740 EM, Penalva LO. 2010. Sequence signatures and mRNA concentration can explain two-
741 thirds of protein abundance variation in a human cell line. *Mol Syst Biol* **6**: 400.
742 Wang J, Bai Y, Li N, Ye W, Zhang M, Greene SB, Tao Y, Chen Y, Wehrens XHT, Martin JF.
743 2014. Pitx2-microRNA pathway that delimits sinoatrial node development and inhibits
744 predisposition to atrial fibrillation. *Proc Natl Acad Sci U S A* **111**: 9181–9186.
745 Wang Y, Wang J, Gao L, Stamm S, Andreadis A. 2011. An SRp75/hnRNPG complex interacting
746 with hnRNPE2 regulates the 5' splice site of tau exon 10, whose misregulation causes
747 frontotemporal dementia. *Gene* **485**: 130–138.
748 Wethmar K. 2014. The regulatory potential of upstream open reading frames in eukaryotic gene
749 expression. *Wiley Interdiscip Rev RNA* **5**: 765–778.
750 Xue S, Tian S, Fujii K, Kladwang W, Das R, Barna M. 2015. RNA regulons in Hox 5' UTRs
751 confer ribosome specificity to gene regulation. *Nature* **517**: 33–38.
752 Yamamoto H, Unbehaun A, Spahn CMT. 2017. Ribosomal Chamber Music: Toward an
753 Understanding of IRES Mechanisms. *Trends Biochem Sci* **42**: 655–668.
754 Yang R, Weber DJ, Carrier F. 2006. Post-transcriptional regulation of thioredoxin by the stress
755 inducible heterogenous ribonucleoprotein A18. *Nucleic Acids Res* **34**: 1224–1236.
756 Yekta S, Shih I-H, Bartel DP. 2004. MicroRNA-directed cleavage of HOXB8 mRNA. *Science*
757 **304**: 594–596.
758 Zagozewski JL, Zhang Q, Pinto VI, Wigle JT, Eisenstat DD. 2014. The role of homeobox genes

759 in retinal development and disease. *Dev Biol* **393**: 195–208.

760